INSTITUTE OF PHYSICS PUBLISHING JOURNAL OF PHYSICS B: ATOMIC, MOLECULAR AND OPTICAL PHYSICS

J. Phys. B: At. Mol. Opt. Phys. **36** (2003) 1063–1072 PII: S0953-4075(03)55246-4

Spin resonance with trapped ions

Ch Wunderlich[1], **Ch Balzer, T Hannemann, F Mintert, W Neuhauser, D Reiß and P E Toschek**

Institut für Laser-Physik, Universität Hamburg, Jungiusstraße 9, 20355 Hamburg, Germany

E-mail: wunderlich@physnet.uni-hamburg.de

Received 18 October 2002, in final form 16 January 2003
Published 24 February 2003
Online at stacks.iop.org/JPhysB/36/1063

Abstract

A modified ion trap is described where experiments (in particular related to quantum information processing) that usually require optical radiation can be carried out using microwave or radio frequency electromagnetic fields. Instead of applying the usual methods for coherent manipulation of trapped ions, a string of ions in such a modified trap can be treated like a molecule in nuclear magnetic resonance experiments taking advantage of spin–spin coupling. The collection of trapped ions can be viewed as an N-qubit molecule with adjustable spin–spin coupling constants.

Given N identically prepared quantum mechanical two-level systems (qubits), the optimal strategy to estimate their quantum state requires collective measurements. Using the ground state hyperfine levels of electrodynamically trapped $^{171}Yb^{+}$, we have implemented an adaptive algorithm for state estimation involving sequential measurements on arbitrary qubit states.

1. Introduction

The localization and preparation of individual quantum systems is prerequisite for many intriguing experiments on fundamental issues of quantum mechanics. In addition, the ability to manipulate quantum states, for example, of electrodynamically trapped ions is an essential ingredient for quantum information processing (QIP). Considerable experimental progress has been made in recent years concerning well controlled coherent excitation of internal and external (motional) states of trapped ions (documented, for instance, in this special section).

In many experiments with trapped ions, including the ones related to QIP, it is necessary to couple the dynamics of internal and external degrees of freedom. To this end optical radiation is usually employed. Here, we introduce a new concept for a linear ion trap that allows for the addressing and coherent manipulation of individual ions and their motional states using microwave (mw) or radio frequency (rf) radiation. Furthermore, it is shown that a

[1] Author to whom any correspondence should be addressed.

0953-4075/03/051063+10$30.00

collection of N trapped two-level ions in such a new type of trap exhibits pairwise spin–spin coupling between individual ions. This coupling between internal ionic states is mediated by the vibrational modes of the ion string, but does not involve their direct excitation. Its formal description is identical to so-called J-coupling between nuclear spins in molecules. Therefore, schemes designed for coherent conditional dynamics of nuclear spins in molecules can be directly applied to a designed N-qubit 'molecule' in an ion trap.

Important steps towards the experimental realization of conditional dynamics with a collection of ions have been undertaken: virtually decoherence-free single-qubit operations with $^{171}Yb^{+}$ ions are reported where two hyperfine states of the ground state of $^{171}Yb^{+}$ serve as a qubit. Taking advantage of these arbitrary qubit operations a self-learning algorithm for the estimation of unknown quantum states was implemented.

The remainder of this paper is organized as follows: at the beginning of section 2 a brief introduction to basic requirements for QIP with trapped ions is given. In particular, the need to use optical radiation in conventional traps will be accounted for. Then we will show how, in a modified trap, spin resonance experiments with mw or rf radiation become possible, even when internal and motional states need to be coupled. Section 3 is devoted to experiments with trapped $^{171}Yb^{+}$ ions. In particular, the implementation of a self-learning algorithm for state estimation of quantum mechanical two-state systems (qubits) is reported.

2. Basic elements of QIP with trapped ions

2.1. Optical scheme

Two internal states of each ion, labelled $|0\rangle$ and $|1\rangle$ and separated by $\hbar\omega_0$, serve as the elementary physical unit (the qubit) when using a string of ions crystallized in a linear trap for QIP. If the confinement of N ions is much stronger in the radial than in the axial direction, the ions will form a linear chain [1] with inter-ion spacing $\delta z \approx \zeta 2N^{-0.56}$ where $\zeta \equiv (e^2/4\pi\epsilon_0 m\nu_1^2)^{1/3}$, m is the mass of one ion, and ν_1 is the angular vibrational frequency of the axial centre-of-mass (COM) mode of the ion string [2]. The inter-ion spacing, determined by mutual Coulomb repulsion and the external trapping potential, is typically a few micrometres. In order to individually manipulate each qubit, electromagnetic radiation used for coherent excitation must be focused to a spot much smaller than δz. Therefore, radiation in the optical regime has to be used for individually addressing each ion.

It is clear that in order to implement a quantum algorithm, quantum information has to be transferred between qubits, and conditional dynamics with several qubits has to be possible. That is, one qubit changes its state conditioned on the state of other qubits. It has been shown that arbitrary single-qubit operations together with suitable two-qubit gates are sufficient to synthesize any desired quantum algorithm [3]. In a linear Paul trap the vibrational motion of the ion string serves as a 'bus-qubit' to transmit quantum information between individual ions [4]. This means that internal state dynamics needs to be coupled to the external harmonic motion of the ion string. What is the physical origin of the coupling between qubit states and the motion of the harmonic oscillator? Upon absorption or emission of a photon, a free atom (or ion) takes up the momentum $\hbar\vec{k}$ associated with the photon where $k = 2\pi/\lambda$ and λ is the wavelength of the radiation. In a trap an ion can change its external energy only by discrete amounts $\hbar\nu_n$ with ν_n ($n = 1, 2, \ldots, N$) being the angular frequency associated with an axial vibrational mode of the ion string. The Hamiltonian describing the coupling between internal states and a particular vibrational mode is

$$H_I = \tfrac{1}{2}\hbar\Omega_R(\sigma_+ + \sigma_-)[\exp[\mathrm{i}(\eta_n(a_n^\dagger + a_n) - \omega t + \varphi)] + \mathrm{h.c.}], \tag{1}$$

where $\Omega_R = \vec{d} \cdot \vec{F}/\hbar$ is the Rabi frequency with $\vec{d} \cdot \vec{F}$ signifying either magnetic or electric coupling between the atomic dipole and the respective field component. $\sigma_{+,-} = 1/2(\sigma_x \pm \sigma_y)$ are the atomic raising and lowering operators, respectively, $z_n(a^\dagger + a)$ is the position operator ($z_n = \sqrt{\hbar/(2m\nu_n)}$), and φ is the initial phase of the driving field. The Lamb–Dicke parameter (LDP) $\eta = \hbar k/(2p_n)$ (with $p_n = \sqrt{\hbar m \nu_n/2}$) is a measure for the strength of the coupling. If the linewidth of the internal resonance $\Gamma \ll \nu_n$, the ionic resonance at ω_0 will be accompanied by sideband resonances $\omega_0 \pm \nu$ (first order in η_n). Excitation of these sidebands amounts to coupling internal and external dynamics.

The LDP can also be written as $\eta_n = z_n k$, where z_n is a measure for the extension of the ground state wavefunction of the harmonic oscillator ($2z_n^2$ is the variance of the wavefunction). Typically, z_n is of the order 10 nm. In order for η_n to take on an appreciable nonzero value, and therefore to make it possible to excite motional states by irradiating the ion with electromagnetic radiation, wavelengths in the optical regime are required.

Consequently, when using trapped ions for QIP, a considerable part of the experimental effort has to be devoted to the development of light sources suitable for precise coherent driving of ionic resonances. In particular, the coherence time of laser radiation limits the time available for quantum logic operations. If one-photon transitions are used (for example an electric quadrupole transition in Ba^+ or Ca^+ [5–7]), this leads to rather stringent limits on the emission bandwidth that typically has to be of the order $\Delta\omega/\omega \leqslant 10^{-12}$. Generating laser light with long coherence time (i.e. small $\Delta\omega/\omega$) is a challenging task that is also essential for optical frequency standards (see contributions in this special section). Further issues that have to be considered when using light for quantum gates are its frequency stability (low drift) and intensity stability. Furthermore, the transverse beam profile, pointing stability, and diffraction effects have to be well under control to suppress spurious excitation and allow for precise manipulations.

If, instead of one-photon resonances, Raman transitions, for instance, between two hyperfine states are employed [8], then the most stringent requirement for QIP, the small emission bandwidth of laser light, can be fulfilled more easily. However, the other problems associated with the use of optical beams mentioned in the previous paragraph remain. When using Raman transitions *relative* fluctuations between two light beams have to be controlled with high accuracy. This is, in principle, a more amenable task. A more detailed look at the types of ions that have been used for QIP or related experiments reveals that rather intricate optical setups are still necessary, partly requiring laser wavelengths that are not easily accessible and/or a considerable number of laser beams that need to be controlled accurately.

In order to produce two laser beams with a fixed frequency difference (or ideally two phase-locked light sources) for Raman excitation of Zeeman states, rf or mw signals have to be generated, processed, phase locked, and then employed to control the necessary light sources. From the considerations at the beginning of this section it is clear that rf or mw radiation cannot *directly* be used to address individual ions or couple their internal (Zeeman) and external states, and one has to take the diversion via laser light (by imprinting rf signals onto optical beams) to achieve these goals.

2.2. Spin resonance with trapped ions

In spin resonance experiments, for instance nuclear magnetic resonance (NMR), advanced techniques that have been developed over many decades have been successfully used to experimentally demonstrate complete quantum algorithms involving a large number of quantum gates [9]. The technological basis for the sophisticated techniques employed in NMR or electron spin resonance (ESR) is the virtuosic manipulation of rf and mw radiation. A

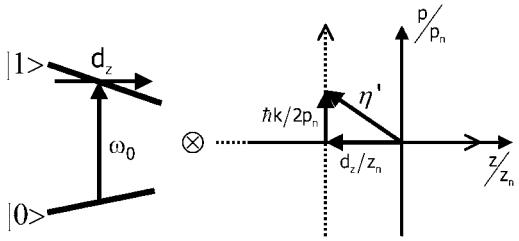

Figure 1. The figure illustrates the coupling of internal and motional states in the presence of a static field gradient. The internal states of an ion (labelled $|0\rangle$ and $|1\rangle$) are Zeeman-shifted as a function of position (left); the external state is indicated in a phase-space diagram (right). An internal transition is accompanied by a shift $dz = -\hbar\partial_z\omega_0/(m\nu_n^2)$ of the equilibrium position of the ion. This may lead to vibrational excitation of the harmonic oscillator even if the momentum transferred to the ion from an absorbed photon is negligible, since the effective LDP is given by $\eta' = \eta - \mathrm{i}\epsilon = \hbar k/2p_n - \mathrm{i}dz/z_n$.

drawback associated with the NMR approach to quantum computing is the use of a macroscopic ensemble that makes the preparation of pseudo-pure states necessary and leads to an exponential decrease in the signal strength as a function of the number of qubits [10]. The use of large ensembles is necessary because the read-out of individual qubits is hard to achieve with the usual spin resonance techniques. Finding, or designing, molecules that have a large number of qubits (nuclear spins) with useful coupling constants also poses some difficulties. Trapped ions, on the other hand, provide us with individually accessible qubits.

The proposal outlined in what follows makes it possible to apply rf or mw radiation to ions in a modified linear trap, allowing for individual addressing and conditional dynamics. Applying a time-independent magnetic field gradient along the axis of a trap individually shifts hyperfine (Zeeman) states, thus making the qubits distinguishable in frequency space [11]. When driving an internal transition of an ion, the dependence of the internal state energy on the position of the ion due to the static field gradient leads to a shift $dz = -\hbar\partial_z\omega_0/(m\nu_n^2)$ in the equilibrium position of the ion. This may lead to the excitation of vibrational motion of the ion string (compare figure 1). At the same time the recoil of the absorbed or emitted photon (on a sideband resonance) results in a kick to the harmonic oscillator along the momentum coordinate which, however, is negligible when using mw radiation, that is, $\eta \approx 0$. A formal description of the interaction between ions and driving radiation shows that the interaction Hamiltonian has the same form as given in equation (1), except that the coupling between internal and external states is now determined by a new effective LDP $\eta' \equiv \eta - \mathrm{i}\epsilon$ where $\epsilon \equiv dz/z_n = z_n\partial_z\omega_0/\nu_n$ [11]. This means that all schemes requiring individual addressing and/or conditional dynamics devised for optical ion experiments can also be applied with such a new type of trap in the rf or mw regime.

All coherent operations are done using mw radiation, whereas for initial (Doppler-)cooling and state selective spin detection laser light driving optical dipole transitions are used. Optical beams for *coherent* manipulation (Raman scheme or one-photon scheme) and sideband cooling are no longer necessary which reduces the potential errors associated with optical beams mentioned in section 2.1 and the number of necessary laser beams. If $^{171}Yb^{+}$ is used with the new scheme presented here, the necessary wavelengths at 369 and 935 nm for cooling and detection can be generated by diode lasers which considerably simplifies the experimental apparatus compared to existing setups as described, for instance, in [6, 8].

Instead of using motional sidebands for conditional dynamics with ions confined in a linear trap with an additional static field gradient, spin–spin coupling between the internal states of

the ions may be used. The Hamiltonian describing a string of N ions in such a trap reads [12]

$$H = \frac{\hbar}{2}\sum_{j=1}^{N}\omega_j(z_{0,j})\sigma_{z,j} + \sum_{n=1}^{N}\hbar\nu_n(a_n^\dagger a_n) - \frac{\hbar}{2}\sum_{i<j}^{N}J_{ij}\sigma_{z,i}\sigma_{z,j}. \tag{2}$$

The first term on the right-hand side of equation (2) is the sum of the internal energies of N two-level ions located at their equilibrium positions $z_{0,j}$. The second term describes N axial vibrational modes with frequencies $\nu_1, \ldots, \nu_N$. The last term indicates pairwise coupling between internal states of the ions where the coupling constants J_{ij} are given by

$$J_{ij} \equiv \sum_{n=1}^{N}\nu_n\epsilon_{ni}\epsilon_{nj}, \qquad \text{and} \tag{3}$$

$$\epsilon_{nj} \equiv S_{nj}\frac{z_n\partial_z\omega_j}{\nu_n}. \tag{4}$$

S_{nj} is the dimensionless entry of the unitary matrix that diagonalizes the dynamical matrix. It is a measure for how much the ion j participates in the motion of the vibrational mode n. Since any quantum mechanical two-level system can be mathematically described as a fictitious spin-1/2, we denote this term as spin–spin coupling.

In molecules used for NMR, different nuclei share binding electrons that generate a magnetic field at the location of the nuclei. The energy associated with the orientation of nuclear spins exposed to the electrons' magnetic field depends on the charge distribution of the binding electrons. If a particular nuclear spin is flipped, the interaction with the surrounding electrons will slightly change the electrons' charge distribution which in turn affects the energy of other nuclear spins. This is, qualitatively, the physical origin of J-coupling between nuclear spins which is used to implement conditional dynamics in NMR experiments. The indirect spin–spin coupling between ionic states in a trap is realized in a different way: the role of the binding electrons as a mediator of the interaction between spins is played here by the vibrational motion of the ion string. Formally the coupling term that arises in the type of ion trap discussed here is identical to the one in molecules, despite the different physical origins. Consequently, the successful techniques and technology developed in spin resonance experiments, like NMR or ESR, can immediately be applied to trapped ions. An advantage of an artificial 'molecule' in a trap is that the coupling constants J_{ij} can be chosen by the experimenter by setting the magnetic field gradient determining $\partial_z\omega_j$, the secular trap frequency ν_1 (and thus $\nu_2, \ldots, \nu_N$), and the type of ion used.

In addition, individual spins can be detected state selectively with an efficiency close to 100% by collecting scattered resonance fluorescence. This is a routine task in ion trap experiments requiring modest specifications of the light sources used for this purpose.

More details on the size of the required field gradients and the coupling constants, and other considerations relevant for an experimental implementation can be found in [7, 11, 12]. This ion 'molecule' concept for QIP is the subject of ongoing detailed theoretical and experimental investigations carried out in our group.

3. Experiments with $^{171}Yb^{+}$

In the experiments reported here, the $S_{1/2}$ ground-state hyperfine doublet of a single $^{171}Yb^{+}$ ion confined in a Paul trap represents the qubit (figure 2). The

$$|0\rangle \equiv |S_{1/2}, F = 0\rangle \leftrightarrow |S_{1/2}, F = 1, m_F = 0\rangle \equiv |1\rangle \tag{5}$$

transition is driven by a mw field close to 12.6 GHz. Resonance fluorescence scattered on the $S_{1/2}(F = 1) \leftrightarrow P_{1/2}$ transition driven by a laser at 369 nm serves for state selective detection

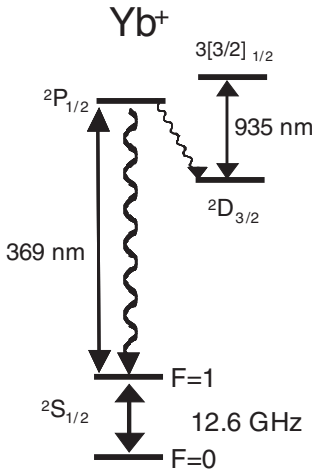

Figure 2. Relevant energy levels of $^{171}Yb^{+}$ (not to scale). The hyperfine doublet serves as a qubit. Scattering of light near 369 nm allows for state selective detection of the hyperfine state $|S_{1/2}, F = 1\rangle$, whereas light near 935 nm avoids optical pumping into the metastable $D_{3/2}$ state.

with efficiency >98%. Optical pumping into the $D_{3/2}$ state is prevented by illuminating the ions with laser light near 935 nm driving the transition $|D_{3/2}, F = 1\rangle \rightarrow |[3/2]_{1/2}\rangle$.

3.1. Coherent manipulation of hyperfine states

Figure 3(a) displays Rabi oscillations between the states $|0\rangle$ and $|1\rangle$. These data were recorded by repeating the following sequence 85 times for a given length τ of the mw pulse.

(i) The ion is prepared by optical pumping in state $|0\rangle$ by illuminating it for 6 ms with light close to 369 nm detuned a few megahertz to the red side of the $S_{1/2}(F = 1) \leftrightarrow P_{1/2}(F = 0)$ resonance.

(ii) A mw pulse of frequency ω and length τ drives the $|0\rangle$–$|1\rangle$ transition. In a frame rotating with ω, that is after transformation of the Hamiltonian according to $A^{\dagger}HA$ with $A = \exp[-i/2(\omega t\sigma_z)]$, the time evolution operator of the driven qubit is $U(t) = \exp[-i/2(\phi\vec{\sigma}\cdot\vec{n})]$ with $\vec{n} = (\Omega_R/\Omega, 0, \delta/\Omega)^T$ where $\delta = \omega_0 - \omega$, $\phi = \Omega t$, Ω_R is the Rabi frequency, and $\Omega = \sqrt{\Omega_R^2 + \delta^2}$. Here $\Omega_R \gg \delta$, and we have $U(t) = \exp[-i/2(\varphi\sigma_x)]$.

(iii) Illuminating the ion again with UV light (369 nm) for 3 ms and simultaneously collecting resonance fluorescence serves for state selective detection.

If scattered light is observed in step (iii), then the ion resides in state $|1\rangle$, otherwise in state $|0\rangle$. The contrast (defined as $1 - \min(P_1(t))/\max(P_1(t))$ with P_1 the excitation probability of state $|S_{1/2}, F = 1\rangle$) of the oscillatory pattern in figure 3(a) is 0.89 in these experimental runs due to imperfect initial preparation of state $|0\rangle$ in step (i). These coherent oscillations indicate that the two-level system, while being driven by mw radiation, shows no detectable decoherence on experimentally relevant timescales.

The results of a Ramsey type experiment are also shown in figure 3. The single mw pulse (step (ii)) of variable length in the procedure used to record Rabi oscillations is replaced by a $\pi/2$ mw pulse preparing the ion in a coherent superposition $1/\sqrt{2}(|0\rangle - i|1\rangle)$. Then this superposition state propagates in time under the Hamiltonian $U(t) = \exp[-i/2(\delta t\sigma_z)]$, that is, it acquires a phase δt relative to the driving field that was initially applied. After time T of

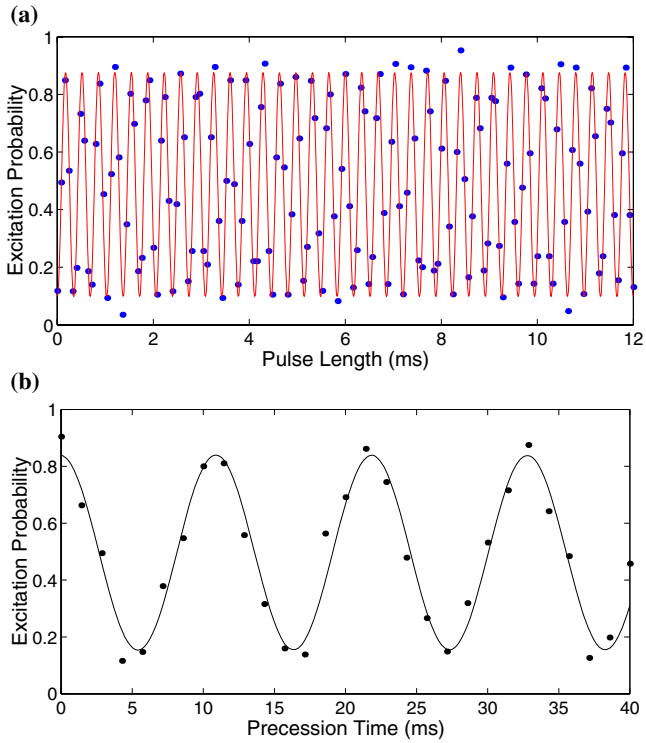

Figure 3. (a) Excitation probability of state $|S_{1/2}, F = 1\rangle$ as a function of mw pulse length applied to a single $^{171}Yb^{+}$ ion: the hyperfine qubit exhibits Rabi oscillations with frequency $2917 \times 2\pi$ Hz. Each datum represents the average of 85 realizations. (b) Excitation probability of state $|S_{1/2}, F = 1\rangle$ as a function of the time between two $\pi/2$-pulses during which the $^{171}Yb^{+}$ ion undergoes free precession (100 repetitions). The detuning $\delta = \omega_0 - \omega$ determined from the Ramsey interference fringes is 91.3 Hz. The sub-unity contrast in both experiments is determined by imperfect initial preparation of state $|S_{1/2}, F = 0\rangle$.

(This figure is in colour only in the electronic version)

free precession, the coherent superposition is interrogated again by a second $\pi/2$ mw pulse, followed by a light pulse close to 369 nm (step (iii)) for state selective detection. Thus, the Ramsey interference fringes displayed in figure 3 are obtained. Again, the contrast is limited only by the imperfection of the initial preparation of state $|0\rangle$. This experiment demonstrates that the hyperfine qubit does not suffer from detectable decoherence during free propagation.

3.2. Adaptive estimation of quantum states

The notion of a quantum state, mathematically represented by an element in Hilbert space, is central to quantum theory. How can the state of a system described by quantum mechanics be determined? Taking advantage of tomographic methods, for instance, quantum states of light fields and motional states of atoms and ions have been reconstructed [13]. Here we are interested in the state estimation of quantum mechanical two-state systems (qubits) and investigate how maximal information about an unknown qubit state can be gathered. In [14] two identically prepared qubits were considered and it was strongly suggested (and later proven in [15]) that optimal information gain about the qubits' state requires a *simultaneous*

measurement on both qubits in an entangled basis. This means that by transferring quantum information between the two qubits, more information (in [14] the Shannon entropy was used as a measure for information) about their state can be extracted than if only local operations and classical communication were used. In further theoretical work optimal and minimal measurement strategies have been found for the estimation of qubit states when more than $N = 2$ identically prepared qubits are available [16]. Optimal schemes always require measurements in an entangled N-qubit basis. This requirement makes it not only experimentally challenging to implement an optimal strategy and test the theoretical predictions, but it is also necessary that all N qubits are available simultaneously.

In [17] an adaptive algorithm for quantum state estimation has been proposed that comes very close to the performance of an optimal scheme, even for a moderate number of available qubits ($N \leqslant 20$). The qubits are measured *sequentially* and the measurement basis of the nth measurement is determined by the outcome of the previous $(n-1)$ measurement ($n = 1, 2, \ldots, N$). We have implemented this adaptive strategy to estimate the state of the hyperfine qubit in $^{171}Yb^{+}$ [18].

The information known about the state of a qubit can be represented by a probability density distribution $w_{n-1}(\theta, \phi)$ on the surface of the Bloch sphere ($\theta \in [0, \pi]$, $\phi \in [0, 2\pi)$ indicate the polar and azimuthal coordinate). The density matrix describing the state is given by

$$\varrho_{n-1} = \int_0^{\pi} \mathrm{d}\theta \sin\theta \int_0^{2\pi} \mathrm{d}\phi \, w_{n-1}(\theta, \phi) |\theta, \phi\rangle\langle\theta, \phi|. \tag{6}$$

Before a measurement is performed, the lack of information on the qubits' state is reflected by a uniform distribution $w_0(\theta, \phi) = 1/4\pi$. After having obtained the measurement outcome $|\theta_m, \phi_m\rangle$ in measurement n, $w_n(\theta, \phi)$ is obtained from $w_{n-1}(\theta, \phi)$ using Bayes rule [19]:

$$w_n(\theta, \phi|\theta_m, \phi_m) = \frac{w_{n-1}(\theta, \phi)|\langle\theta_m, \phi_m|\theta, \phi\rangle|^2}{p_n(\theta_m, \phi_m)}. \tag{7}$$

Considering the knowledge that has been gained in previous measurements ($0, \ldots, n-1$; $n \geqslant 1$), the task is now to optimize the information gain in measurement step n, that is, to determine the optimal basis for the succeeding measurement. To this end, the Shannon entropy $S = -\sum_{x=+,-} p_x \log(p_x)$ can be maximized, where $p_+ = p_n(\theta_m, \phi_m)$ ($p_- = p_n(\bar{\theta}_m, \bar{\phi}_m)$) is the *a priori* probability to measure state $|\theta_m, \phi_m\rangle$ ($|\bar{\theta}_m, \bar{\phi}_m\rangle$). The Shannon entropy measures the uncertainty about the qubit's state before a measurement has been performed, or alternatively, the gain of information after a measurement. It is maximal if both possible outcomes determined by the selected measurement basis have equal probability. The first measurement direction is, of course, arbitrary, since no prior knowledge is available. The second measurement direction has to be perpendicular to the first one in order to maximize S, and the third one perpendicular to the first two. However, for $n \geqslant 4$ the optimal basis depends on all previous $n-1$ measurement outcomes. In numerical simulations the use of the fidelity (as in the remainder of this paper) has been proven to be a better choice to optimize the estimate of an unknown quantum state [17].

After measurement $n-1$ one obtains the probability density function $w_{n-1}(\theta, \phi)$ that determines ρ_{n-1}. The state $|\theta', \phi'\rangle$ having maximal overlap with this density operator maximizes the fidelity

$$F_{n-1}(\theta', \phi') = \langle\theta', \phi'|\rho_{n-1}|\theta', \phi'\rangle. \tag{8}$$

If in the next measurement n the basis determined by (θ_m, ϕ_m) were used, and the result of the measurement were $|\theta_m, \phi_m\rangle$, then the estimated state after measurement n would be obtained

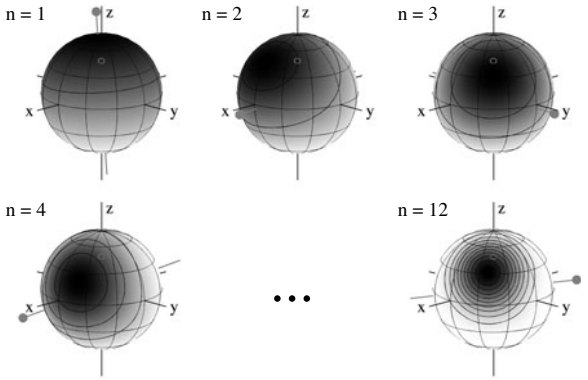

Figure 4. A sequence of $N = 12$ adaptive measurements carried out on identically prepared qubits in order to estimate their state ($|\pi/4, \pi/4\rangle$, marked by a grey circle). The probability density $w_n(\theta, \phi)$ is greyscale coded on the surface of the Bloch sphere (the greyscale code is different for each measurement). In addition, contour lines indicate where w_n takes on the values 0.1, 0.2, ... A grey straight line through each Bloch sphere shows the measurement direction and the filled grey circle indicates the measurement outcome. The fidelity of state estimation of this particular run is 98.2%.

by maximizing the fidelity $F_n(\theta', \phi'|\theta_m, \phi_m)$, that is, from

$$F_n^{\text{opt}}(\theta_m, \phi_m) = \max[F_n(\theta', \phi'|\theta_m, \phi_m)] \tag{9}$$

by varying θ', ϕ'. However, the nth the measurement may as well have the outcome $|\bar{\theta}_m, \bar{\phi}_m\rangle$). Therefore, the optimal fidelity for the measurement direction (θ_m, ϕ_m) is obtained by the weighted sum

$$\bar{F}_n(\theta_m, \phi_m) = p_n(\theta_m, \phi_m) F_n^{\text{opt}}(\theta_m, \phi_m) + p_n(\bar{\theta}_m, \bar{\phi}_m) F_n^{\text{opt}}(\bar{\theta}_m, \bar{\phi}_m) \tag{10}$$

(the weights p_n are the probabilities for each of the two possible measurement outcomes.) Maximizing $\bar{F}_n(\theta_m, \phi_m)$ as a function of θ_m, ϕ_m then gives the desired result [18].

In figure 4, probability density distributions are displayed that have been obtained from a single experimental run of $N = 12$ consecutive measurements of the hyperfine qubit in $^{171}Yb^+$ in order to estimate its state. The initially prepared state $|\theta = \pi/4, \phi = \pi/4\rangle$ to be estimated is marked with a circle on the surface of the Bloch sphere. The grey straight lines show the measurement directions n and the filled circles indicate the measurement outcome. Four different initial states were estimated ($|\pi/4, \pi/4\rangle$, $|\pi/4, 3\pi/4\rangle$, $|3\pi/4, \pi/4\rangle$, $|3\pi/4, 3\pi/4\rangle$), each of them 100–200 times. The average experimental fidelity $85.0 \pm 0.6\%$ agrees well with the average theoretical value $85.4 \pm 0.7\%$ obtained from simulating the adaptive algorithm 10^4 times taking into account the experimentally determined preparation and detection efficiencies.

The performance of the self-learning algorithm has been compared, among others, to state estimation using a randomly chosen measurement basis in each of the N steps. The experimental and theoretical average fidelity for $N = 12$ randomly distributed measurements is 81.9 ± 0.6 and $81.9 \pm 0.7\%$, respectively. The difference between the two methods under experimental conditions, that is, including decoherence due to initial preparation and detection, turns out to be larger than under ideal decoherence free conditions. A detailed comparison with other estimation schemes employing a fixed set of measurement basis will be published elsewhere.

The estimation procedure implemented here allows for separate (local) measurements on each qubit (a total of N identically prepared qubits are available). Following each measurement

on a particular qubit, classical information is used to determine the best measurement to be performed on the next qubit. In [20] the optimal LOCC scheme (performing local operations with exchange of classical information) is introduced for arbitrary states on the Bloch sphere (3D case). Interestingly, if the state to be estimated lies in the xy-plane (2D case), then local operations alone suffice to obtain the optimal state estimate, and classical communication is not necessary. This optimal LO(CC) scheme exhibits the same asymptotic behaviour with the number N qubits as the optimal scheme taking advantage of collective measurements, and yields a slightly better average fidelity than the adaptive scheme presented here.

Acknowledgments

We gratefully acknowledge financial support from the Deutsche Forschungsgemeinschaft and the Bundesministerium für Bildung und Forschung.

References

[1] Schiffer J P 1993 *Phys. Rev. Lett.* **70** 818
Dubin D H E 1993 *Phys. Rev. Lett.* **71** 2753
[2] Steane A 1997 *Appl. Phys.* B **64** 623
James D F V 1998 *Appl. Phys.* B **66** 181
[3] DiVincenzo D P 1995 *Phys. Rev.* A **51** 1015
Barenco A, Bennett C H, Cleve R, DiVincenzo D P, Margolus N, Shor P, Sleator T, Smolin J A and Weinfurter H 1995 *Phys. Rev.* A **52** 3457
[4] Cirac J I and Zoller P 1995 *Phys. Rev. Lett.* **74** 4091
Sorensen A and Molmer K 2000 *Phys. Rev.* A **62** 022311/1
Jonathan D, Plenio M B and Knight P L 2000 *Phys. Rev.* A **62** 042307
[5] Appasamy B, Stalgies Y and Toschek P E 1998 *Phys. Rev. Lett.* **80** 2805
[6] Roos C, Zeiger T, Rohde H, Nägerl H, Eschner J, Leibfried D, Schmidt-Kaler F and Blatt R 1999 *Phys. Rev. Lett.* **83** 4713
Barton P A, Donald C J S, Lucas D M, Stevens D A, Steane A M and Stacey D N 2000 *Phys. Rev.* A **62** 032503
[7] Wunderlich Ch and Balzer Ch 2003 *Advances in Atomic, Molecular and Optical Physics* (San Diego, CA: Academic) at press
[8] Monroe C, Meekhof D M, King B E, Itano W M and Wineland D J 1995 *Phys. Rev. Lett.* **75** 4714
Wineland D J, Monroe C, Itano W M, Leibfried D, King B E and Meekhof D M 1998 *J. Res. Natl Inst. Stand. Technol.* **103** 259
[9] Vandersypen L M K, Steffen M, Breyta G, Yannoni C S, Sherwood M H and Chuang I L 2001 *Nature* **414** 883
[10] Jones J A 2000 *Fortschr. Phys.* **48** 909
[11] Mintert F and Wunderlich Ch 2001 *Phys. Rev. Lett.* **87** 257904
[12] Wunderlich Ch 2001 *Laser Physics at the Limit* (Berlin: Springer) pp 261–71
[13] Freyberger M, Bardroff P, Leichtle C, Schrade G and Schleich W 1997 *Phys. World* **10** 41
[14] Peres A and Wootters W 1991 *Phys. Rev. Lett.* **66** 1119
[15] Massar S and Popescu S 1995 *Phys. Rev. Lett.* **74** 1259
[16] Derka R, Bužek V and Ekert A K 1998 *Phys. Rev. Lett.* **80** 1571
Latorre J I, Pascual P and Tarrach R 1998 *Phys. Rev. Lett.* **81** 1351
Bagan E, Baig M, Brey A and Munoz-Tapia R 2000 *Phys. Rev. Lett.* **85** 5230
[17] Fischer D G, Kienle S H and Freyberger M 2000 *Phys. Rev.* A **61** 032306
[18] Hannemann T, Reiß D, Balzer C, Neuhauser W, Toschek P E and Wunderlich Ch 2002 *Phys. Rev.* A **65** 050303(R)/1
[19] Bayes T 1763 *Phil. Trans. R. Soc.* **53** 370
Bayes T 1958 *Biometrika* **45** 293
See also, for instance
Ballentine L E 1998 *Quantum Mechanics* (Singapore: World Scientific) ch 1
[20] Bagan E, Baig M and Munoz-Tapia R 2002 *Preprint* quant-ph/0205026